An Investigation of the Generality of Incomplete Transformation to Bainite in Fe-C-X Alloys

W.T. REYNOLDS, Jr., S.K. LIU, F.Z. LI, S. HARTFIELD, and H.I. AARONSON

The overall kinetics of the isothermal transformation of austenite to bainite and to pearlite in high-purity Fe-C-3 at. pct X alloys (X = Mn, Si, Ni, or Cu) containing 0.1 wt pct C and 0.4 wt pct C were investigated with quantitative metallography and transmission electron microscopy (TEM) to ascertain the presence or absence of the incomplete reaction phenomenon. The incomplete transformation of austenite to bainite was not observed in the Fe-C-Si, Fe-C-Ni, Fe-C-Cu, or Fe-0.4C-Mn alloys. It was found, however, in the Fe-0.1C-Mn alloy. Transmission electron microscopy results indicate that sympathetic nucleation of ferrite without carbide precipitation is a necessary but not a sufficient condition for the development of the incomplete reaction phenomenon. Transformation resumes following stasis in the low-carbon Fe-C-Mn alloy with the formation of a nodular bainite. The results support the view that the incomplete transformation of austenite to bainite is a characteristic of specific alloying elements and is not an inherent trait of the bainite reaction.

I. INTRODUCTION

THE bainite reaction has been the subject of extensive research since the 1930s. Because early studies[1,2] of the structure of bainite in steel were hampered by difficulties encountered in resolving the fine structure of the transformation product with optical microscopy, much emphasis was soon placed upon characterizing the kinetic features of the bainite reaction. This approach led to the view that the overall reaction kinetics of bainite are characterized by several salient features.[3,4] Bainite has its own C-curve on a time-temperature-transformation (TTT) diagram distinct from the C-curve for the pearlite reaction. The highest temperature of the bainite C-curve, or the B_s (bainite start) temperature, is the maximum temperature of bainite formation; this temperature is usually well below that of the eutectoid temperature. At reaction temperatures just below the B_s, isothermal transformation of austenite to bainite is incomplete. The fraction of the parent austenite which transforms to bainite increases with decreasing reaction temperature from zero at the B_s to unity at the B_f (bainite finish) temperature. Below the B_f, austenite can transform to 100 pct bainite. Early work on the bainite reaction based upon this view is reviewed in Reference 5; another generation of work is included in the review of Reference 4; more recent summaries are available in References 6 and 7; and brief current reviews are offered in the two preceding papers in these proceedings,[8,9] with a more comprehensive overview being provided in the first paper published in this group.[10]

It should be noted that the foregoing description of bainite, sometimes called the overall reaction kinetics definition,[4] is one of three definitions in current use.[7] In the surface relief definition, bainite consists of ferrite plates that exhibit an invariant plane strain surface relief; this description will not be used here. Microstructurally defined, bainite is any nonlamellar eutectoid decomposition product.[7] To avoid confusion, the term "bainite" will refer here to the transformation product *expected* to follow the overall reaction kinetics definition; this product consists of ferrite with or without carbides but excludes the alternating ferrite and carbide lamellae comprising pearlite. The term "microstructural bainite" will be reserved to describe the nonlamellar mixtures of ferrite and carbide.

The partial transformation of austenite to bainite at temperatures between the B_s and B_f, termed the incomplete reaction phenomenon or transformation stasis, has been documented in alloy steels containing various amounts of Mn, Ni, and Cr, sometimes singly but more often in combination.[11–16] Transformation stasis in steel may be defined as cessation of transformation prior to the appearance of the proportion of ferrite allowed by application of the Lever Rule to the metastable $\alpha + \gamma$ region.[17] Although it is not always found in plain carbon steels, the incomplete reaction phenomenon usually is regarded as an inherent characteristic of the bainite reaction. The inability to observe incomplete transformation in low-alloy steels is generally attributed to the overlap of the pearlite and bainite C-curves. When the two reactions occur simultaneously at a given temperature, the incomplete nature of the bainite reaction is said to be obscured by the formation of pearlite.[3,14,18]

W.T. REYNOLDS, Jr., formerly Graduate Student, Department of Metallurgical Engineering and Materials Science, Carnegie Mellon University, is Assistant Professor, Department of Materials Engineering, Virginia Polytechnic Institute, Blacksburg, VA 24061-0237. S.K. LIU, formerly Visiting Professor, Department of Metallurgical Engineering and Materials Science, Carnegie Mellon University, is Professor and Head, Department of Mechanical Engineering, Southwestern Jiaotong University, Emei, Sichuan, People's Republic of China. F.Z. LI, Visiting Professor, is with the Department of Metallurgical Engineering and Materials Science, Carnegie Mellon University. S. HARTFIELD, formerly Undergraduate Student, Department of Metallurgical Engineering and Materials Science, Carnegie Mellon University, is Graduate Student, Department of Materials and Metallurgical Engineering, University of Michigan, Ann Arbor, MI 48109. H.I. AARONSON, R.F. Mehl Professor, is with the Department of Metallurgical Engineering and Materials Science, Carnegie Mellon University, Pittsburgh, PA 15213-3890.

This paper is based on a presentation made in the symposium "International Conference on Bainite" presented at the 1988 World Materials Congress in Chicago, IL, on September 26 and 27, 1988, under the auspices of the ASM INTERNATIONAL Phase Transformations Committee and the TMS Ferrous Metallurgy Committee.

An alternate view of the incomplete transformation phenomenon maintains that transformation stasis is not a characteristic peculiar to a bainitic transformation mechanism but is instead a special effect of certain alloying elements upon the proeutectoid ferrite reaction in steel.[7] These elements affect the overall transformation kinetics by altering ferrite nucleation kinetics[19] and by reducing ferrite growth kinetics through a solute drag-like effect (SDLE).[7,9,20,21] In its present form, the latter effect is proposed to result from a nonequilibrium concentration of the substitutional solute element (hereafter termed X) and of the interstitial solute, carbon, within moving ferrite:austenite boundaries. These concentrations affect the migration kinetics of the boundaries by changing the carbon concentration (or more precisely, chemical potential) gradient in austenite controlling the diffusional growth of ferrite.[9] The most direct evidence for an SDLE consists of anomalously slow ferrite growth kinetics in Fe-C-X alloys when X is Mo, Mn, or Cr.[20,21,22] It has been suggested that transformation stasis occurs when the SDLE is strong enough to eliminate the concentration gradient driving ferrite growth.[23] In a companion paper,[9] this situation is deduced to be encouraged when extensive sympathetic nucleation of ferrite at $\alpha:\gamma$ boundaries shortens the carbon diffusion distances in austenite required for extensive overlap of diffusion fields associated with nearby ferrite crystals, thereby strengthening the SDLE.[9]

A key aspect of the SDLE hypothesis is that the strength of the "drag" during growth depends upon the character of the X element as well as upon the composition of the $\alpha:\gamma$ boundary. Elements which depress the activity of carbon are expected to reduce the C gradient in austenite and thus the growth kinetics of ferrite. Without the restriction on ferrite growth imposed by the SDLE, transformation stasis is not expected.

This investigation was undertaken to test these opposing views of the incomplete transformation phenomenon by ascertaining whether transformation stasis is general (as predicted by the overall reaction kinetics description of bainite) or peculiar to steels containing certain alloying elements. Quantitative metallography was employed to follow the progress of the bainite transformation in a number of high-purity Fe-C-X systems. Ternary alloys were chosen to avoid the possible complication of interactions among multiple alloying elements. The X solutes selected for study were Mn, Ni, Cu, and Si. These elements have interaction energies with carbon which range from negative to positive values[24,25] and should thus include examples of alloys with and without an SDLE.

II. EXPERIMENTAL PROCEDURE

The compositions of the steels employed in this investigation are shown in Table I. Two carbon levels were selected for study. Low-carbon alloys (approximately 0.1 wt pct C) were chosen to minimize interference from the pearlite reaction and to allow bainite transformation kinetics measurements to be extended to higher reaction temperatures. The higher carbon alloys (approximately 0.4 wt pct C) were employed because C has been observed to enhance the development of transformation stasis in Fe-C-Mo alloys.[9] A concentration of roughly 3 at. pct X (with one exception) was employed to facilitate comparisons among the alloy systems. A concentration of 6.82 at. pct Ni (7.25 wt pct Ni) was used in the high-carbon Fe-C-Ni alloy, because Ni suppresses pearlite formation[26,27] and a published TTT diagram of a similar alloy shows a "notch," or shallow bay, in the diagram at approximately 420 °C.[28] According to conventional wisdom,[4] the incomplete transformation phenomenon should be easier to detect in alloys whose TTT diagrams exhibit a bay.

The alloys were prepared in the manner described in Reference 9. Coupons 10 × 10 × 0.5 mm in size were austenitized at 1300 °C (the 7.25 wt pct Ni alloy was austenitized at 1100 °C) for 900 seconds in a deoxidized salt bath[29] and isothermally reacted in deoxidized Pb before quenching in iced brine. The high austenitization temperature was used to produce a large austenite grain size. This preferentially inhibits the pearlite reaction[3,30] by encouraging the development of intragranular ferrite and reducing the number of favorable sites for pearlite nucleation.[31] The progress of the overall transformation was measured by point counting[32,33] the microstructure of specimens isothermally reacted for successively longer times. The metallographic procedure is described in detail in Reference 34. The transformed fraction of austenite was then plotted as a function of the logarithm of the reaction time; transformation stasis was taken to occur if the fraction transformed to bainite remained constant, within the limits of the experimental technique, at a level significantly below the metastable equilibrium proportion of ferrite.

Specimens from representative alloys, reacted for selected transformation times and temperatures, were examined with transmission electron microscopy (TEM)

Table I. Fe-C-X Alloy Compositions

Wt Pct C	At. Pct C	Wt Pct X	At. Pct X	Wt Pct Mn	Wt Pct Si	Wt Pct P	Wt Pct S
0.10	0.46	2.99Mn	3.03Mn	—	0.02	0.004	0.005
0.38	1.74	3.11Mn	3.12Mn	—	0.03	0.001	0.009
0.11	0.50	1.83Si	3.56Si	<0.002	—	0.002	0.007
0.38	1.71	1.73Si	3.34Si	<0.002	—	0.001	0.006
0.12	0.56	3.28Ni	3.11Ni	<0.002	0.001	0.001	0.004
0.42	1.93	7.25Ni	6.82Ni	<0.01	<0.004	0.001	0.006
0.41	1.89	3.01Cu	2.62Cu	<0.002	0.002	0.002	0.008

to ascertain the presence or absence of carbides at various stages of transformation. Thin foil specimens were prepared by jet polishing in a 30 pct HNO_3, 70 pct methanol solution at −50 °C and 10 to 20 V. Observations were carried out in a JEM 120CX operated at 120 kV.

III. RESULTS

A. *Fe-C-Si*

The isothermal transformation kinetics of the Fe-0.38 wt pct C-1.73 wt pct Si alloy at four reaction temperatures are presented in Figure 1 as curves of the percent of austenite transformed *vs* the logarithm of the reaction time.[35] The transformation product formed at the three lower temperatures, 495 °C, 450 °C, and 395 °C, consisted solely of bainite. The reaction at these temperatures is complete (Figures 1(c) through (e)). Transformation proceeds smoothly from 0 to 100 pct with no indication of transformation stasis. At 560 °C, the highest temperature investigated for this alloy, bainite and pearlite form concurrently. The two reaction products were point counted separately and their transformation curves are shown in Figure 1(a). Figure 1(b) shows the transformation curve for bainite together with the transformation curve for bainite and pearlite combined. The amount of austenite transformed to bainite increases steadily until all of the parent austenite is consumed. The bainite reaction does not exhibit the incomplete reaction phenomenon at this temperature, at least not before approximately half of the austenite transforms to bainite. Thus, nothing that could be interpreted as the incomplete transformation phenomenon is found between 560 °C and 395 °C in this alloy. An example of the morphology of the transformation products formed at 560 °C is shown in the optical micrograph in Figure 2(a) and in the TEM micrograph in Figure 2(b). The bainite has an acicular morphology and consists (in the overall reaction kinetics definition!) of carbide-free ferrite; the dark-etching constituent is pearlite. Although pearlite eventually envelops ferrite, the ferrite tends to form in regions free of pearlite (Figure 2(a)). The separation between the two constituents precludes the possibility that the precipitation of pearlite is altering the composition of the parent austenite in the vicinity of a significant proportion of the ferrite crystals and is thereby interfering with the development of transformation stasis.

The isothermal transformation curves for the Fe-0.11 wt pct C-1.83 wt pct Si alloy are shown in Figure 3. Pearlite nodules are not observed at any of the temperatures investigated (see, for example, Figure 4). In all cases, the bainite transformation proceeds rapidly until approximately 95 pct of the austenite is transformed. This fraction of bainite is within 1.5 pct of the metastable equilibrium fraction of ferrite calculated using the Hillert-Staffansson thermodynamic model[36] on the paraequilibrium* assumption. Thus, cessation of bainite formation at approximately 95 pct transformation is not incomplete transformation. The remaining austenite transforms in about 100 seconds or less. At 528 °C, transformation is too rapid for the early stage to be observed with the present experimental technique. No indication of transformation stasis was detected at temperatures between 675 °C and 528 °C in the Fe-0.11 wt pct C-1.83 wt pct Si alloy.

*Paraequilibrium refers to the constrained equilibrium in which carbon atoms are permitted to partition and equilibrate between ferrite and austenite while the ratio of the atom fraction of substitutional alloying elements to that of iron is the same in ferrite as in austenite.[37,38]

B. *Fe-C-Ni*

The transformation curves of the Fe-0.42 wt pct C-7.25 wt pct Ni alloy at 440 °C, 420 °C, and 400 °C, temperatures in the vicinity of a small bay in the TTT diagram,[28] are shown in Figure 5. A substantial amount of time elapses before the transformation begins, but once initiated, it quickly proceeds to completion. The transformation curves exhibit none of the characteristics of the incomplete transformation phenomenon. The reaction product has an acicular, dark-etching characteristic under optical microscopy (Figure 6), and sideplates originating at austenite grain boundaries are common.

The transformation kinetics in the Fe-0.12 wt pct C-3.28 wt pct Ni alloy are quite rapid (Figures 7(a) and (b)), but again, there is no indication of incomplete transformation. The bainite has an acicular morphology (Figure 8(a)). Pearlite is absent, and a ferrite + carbide mixture (nodular bainite under a recently proposed microstructural classification scheme)[39,40,41] evolves in the austenite regions between the ferrite sideplates. The carbides appear as rows perpendicular to the growth direction of the nodular mixture (Figure 8(b)). The ferrite sideplates are essentially carbide-free (Figure 8(c)).

C. *Fe-C-Cu*

The pearlite reaction was particularly competitive with the bainite reaction in the Fe-0.41 wt pct C-3.01 wt pct Cu alloy. Although the latter reaction was complete at 450 °C (Figure 9(c)), at 500 °C (Figure 9(b)), it comprised 70 pct of the total microstructure, and at 550 °C, it comprised less than 10 pct of the microstructure. Even so, there was no indication that the bainite reaction at 550 °C or 500 °C ceased prematurely. Bainite precipitation initiated at austenite grain boundaries and well-formed sideplates (Figure 10(a)) were common at each temperature. Carbides, whose size and morphology are consistent with those of cementite, were observed both within and between the ferrite plates (Figure 10(b)).

D. *Fe-C-Mn*

Transformation at the upper temperatures of the bainite reaction in Fe-0.38 wt pct C-3.11 wt pct Mn[35] is also complicated by the more or less simultaneous precipitation of pearlite. At 495 °C, bainite and pearlite transform austenite in a competitive fashion (Figure 11(a)); as in the case of the Si- or Cu-containing alloys, the volume of the bainite constituent increases until all of the parent austenite is consumed (Figure 11(b)). At lower temperatures, where bainite is the only transformation product present, the bainite reaction is complete[35] (Figures 11(c) and (d)). The morphology of the ferritic

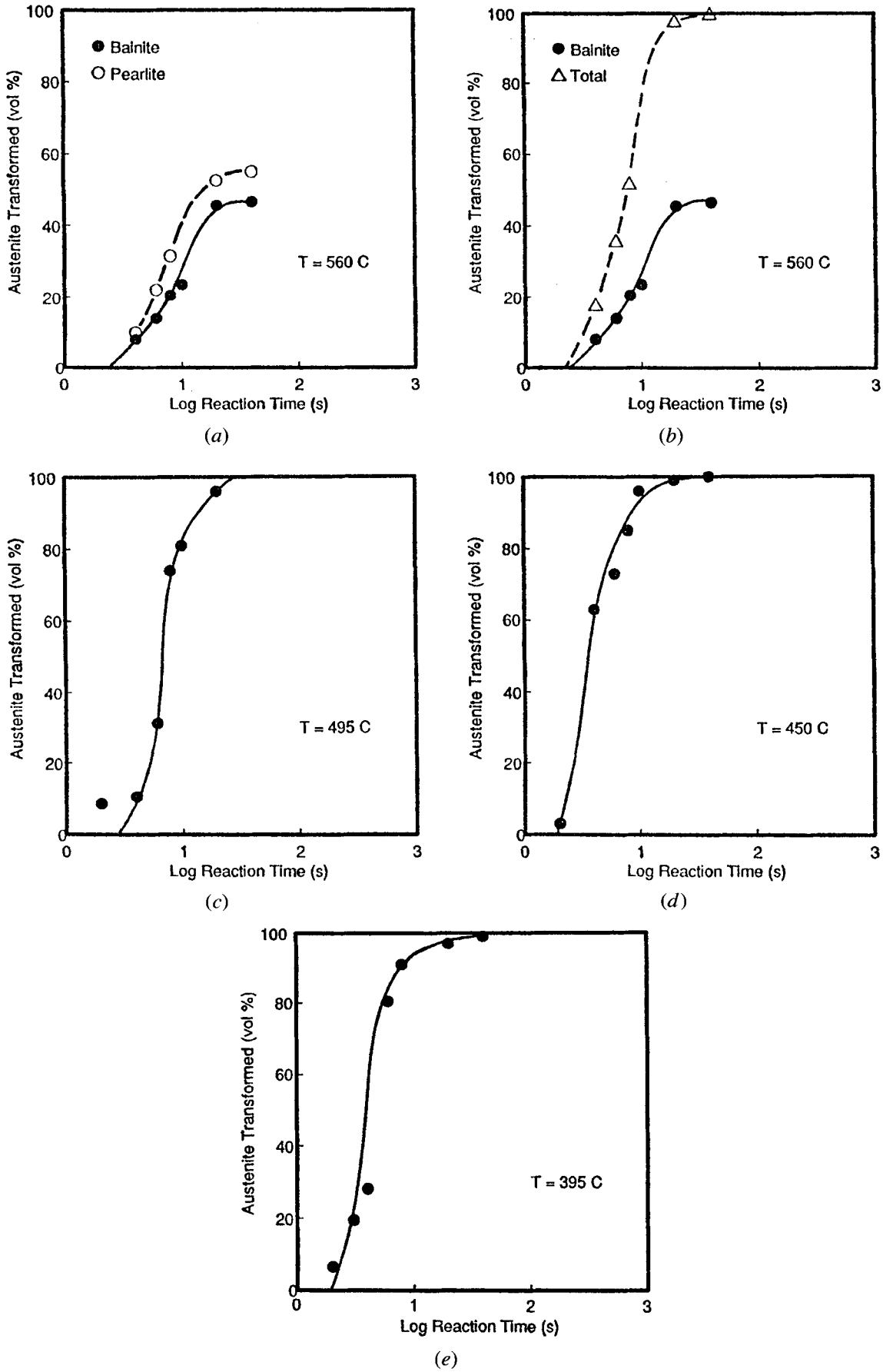

Fig. 1—Isothermal transformation curves for Fe-0.38 wt pct C-1.73 wt pct Si:[35] (*a*) bainite and pearlite, transformed at 560 °C; (*b*) bainite and total austenite reacted, transformed at 560 °C; (*c*) bainite, transformed at 495 °C; (*d*) bainite, transformed at 450 °C; and (*e*) bainite, transformed at 395 °C.

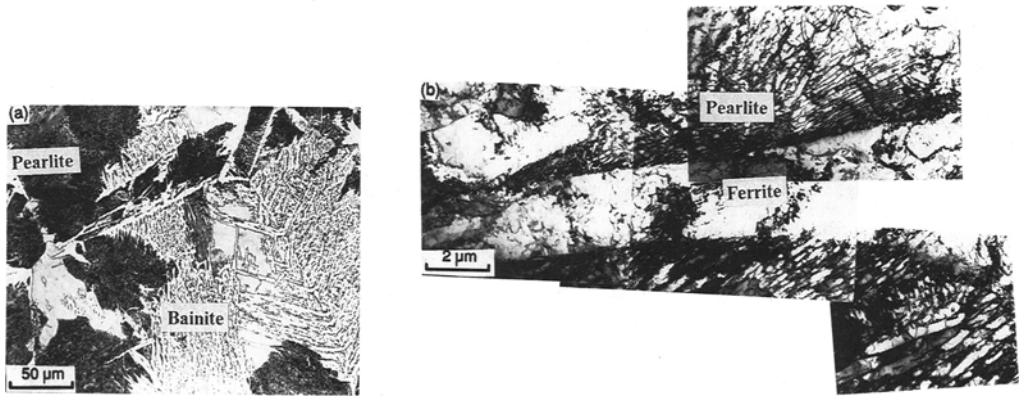

Fig. 2—Fe-0.38 wt pct C-1.73 wt pct Si, transformed at 560 °C: (*a*) 20 s, optical microstructure (2 pct nital etch) and (*b*) 14 s, TEM microstructure.

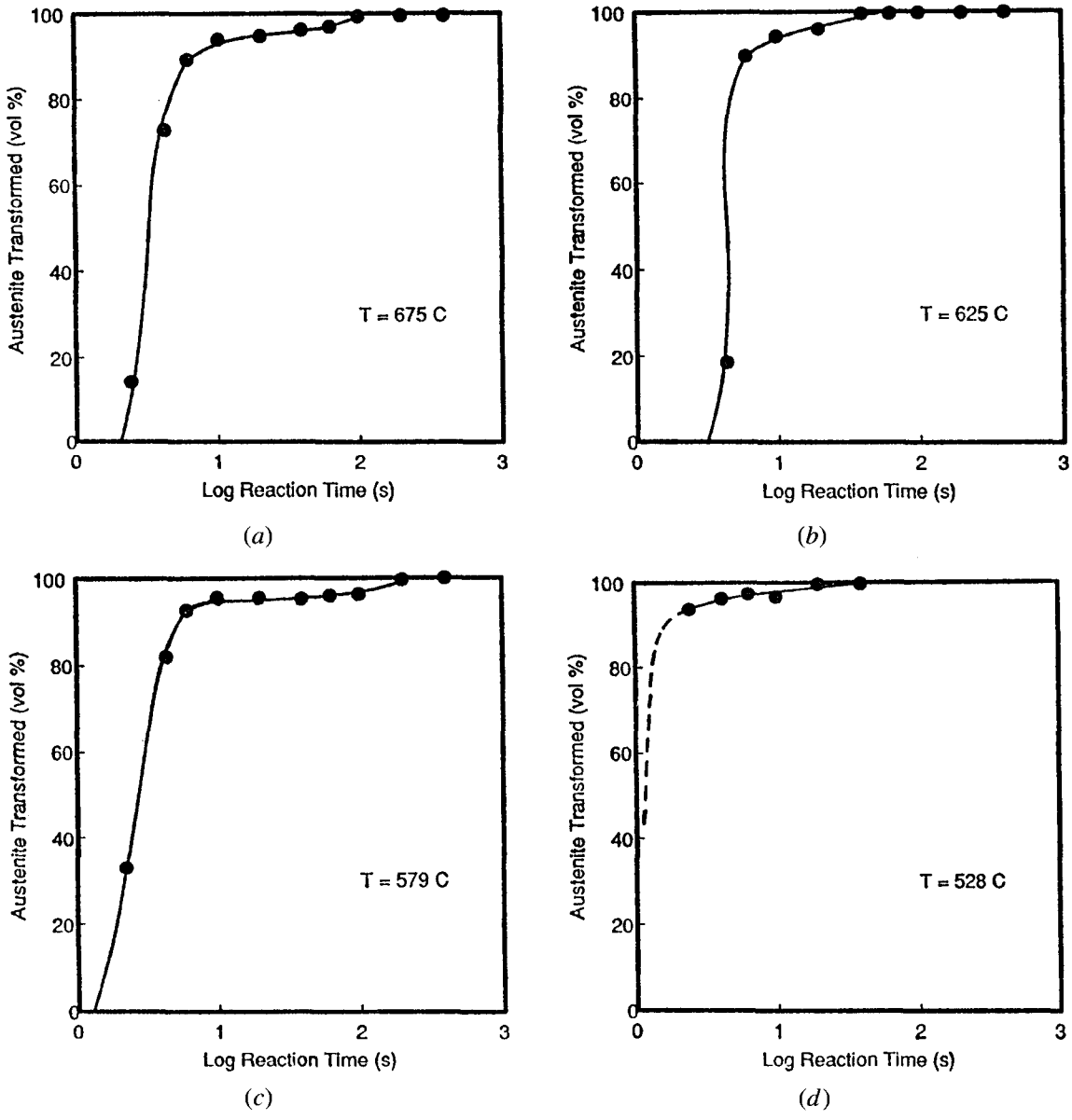

Fig. 3—Isothermal transformation curves for Fe-0.11 wt pct C-1.83 wt pct Si: (*a*) bainite, transformed at 675 °C; (*b*) bainite, transformed at 625 °C; (*c*) bainite, transformed at 579 °C; and (*d*) bainite, transformed at 528 °C.

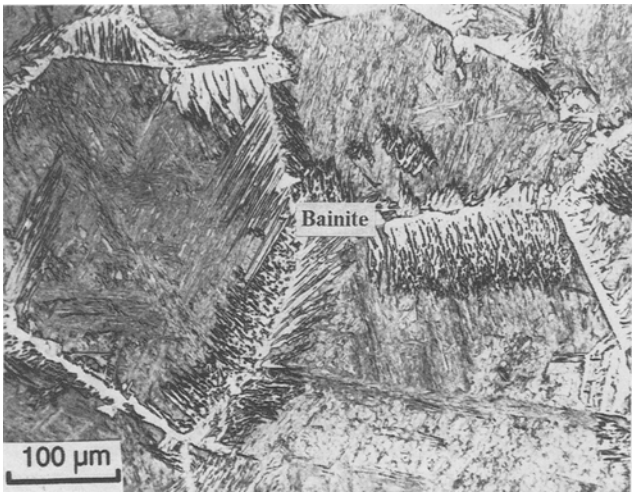

Fig. 4—Fe-0.11 wt pct C-1.83 wt pct Si, transformed at 675 °C, 2 s, optical microstructure (saturated picral etch).

component of bainite consists of sympathetically nucleated sheaves (Figures 12(a) and (b)).[42,43,44] Ferrite sideplates are relatively scarce.

The behavior of the Fe-0.10 wt pct C-2.99 wt pct Mn alloy is substantially different from that of the alloys considered previously. At 600 °C, decomposition of austenite is exceedingly slow (Figure 13(a)). Ferrite allotriomorphs precipitate on austenite grain boundaries but grow very slowly. The sluggish transformation kinetics at high temperatures have been attributed to Mn partitioning during ferrite growth and to the low diffusivity of Mn relative to that of C in austenite.[45] Manganese partitioning during ferrite growth at high reaction temperatures in Fe-C-Mn has been observed in similar alloys[46,47] and is probably responsible for the slow growth kinetics at 600 °C, even though interfacial diffusion of Mn may have accelerated somewhat the growth processes.[47]

Transformation stasis is observed at 550 °C. The transformation curve at this temperature exhibits three stages: an initial stage during which the volume fraction of bainite rapidly increases, a second stage during which little or no bainite forms, and a third stage which completes the transformation of austenite (Figure 13(b)). The increase in the amount of transformation product during the first stage is associated with the precipitation of small crystals of sympathetically nucleated ferrite (Figure 14(a)). Carbides are not present during this stage (Figure 14(c)). The microstructure is qualitatively the same as structures observed in Fe-C-Mo alloys during transformation stasis.[9] The resumption of transformation with the third stage is associated with the precipitation of a eutectoid structure, apparently microstructural nodular bainite (Figure 14(b)). The ferrite and cementite portions of this constituent are not lamellar.

Transformation stasis is not observed at the lower reaction temperatures (Figures 13(c) through (e)). At 500 °C, the second stage of transformation does not begin until approximately 80 pct transformation, and the rate of transformation during this period is always finite. At

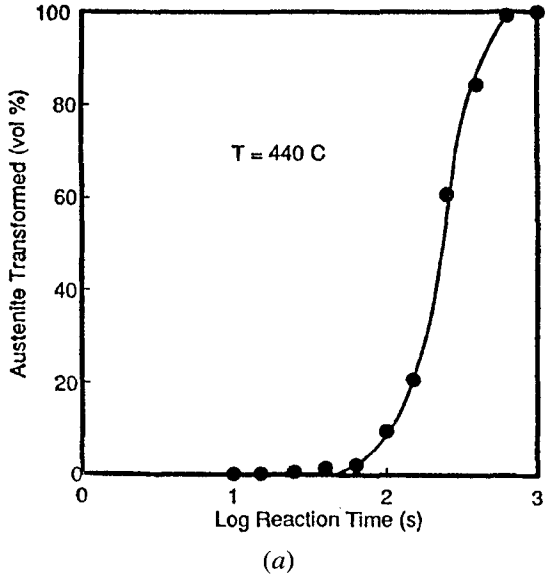

(*a*)

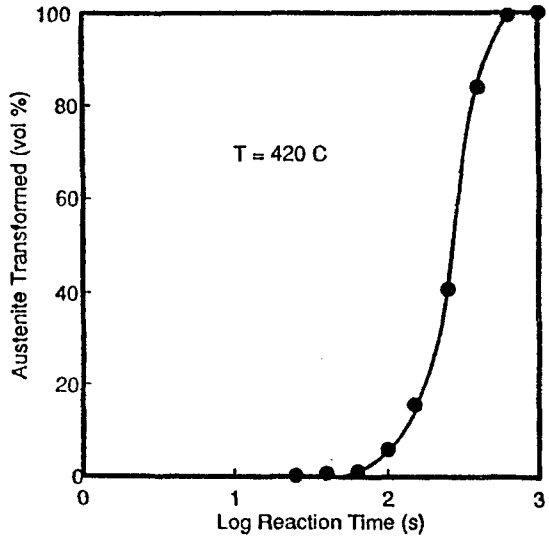

(*b*)

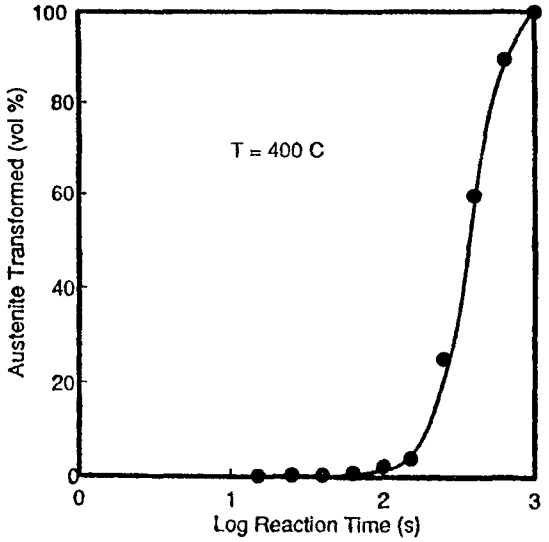

(*c*)

Fig. 5—Isothermal transformation curves for Fe-0.42 wt pct C-7.25 wt pct Ni: (*a*) bainite, transformed at 440 °C; (*b*) bainite, transformed at 420 °C; and (*c*) bainite, transformed at 400 °C.

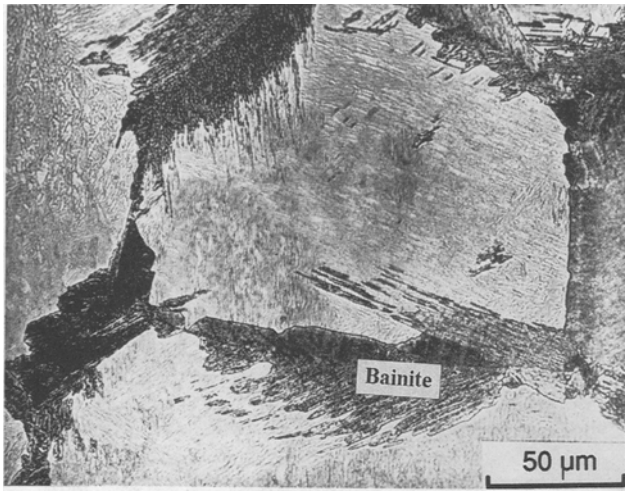

Fig. 6—Optical microstructure of Fe-0.42 wt pct C-7.25 wt pct Ni, transformed at 440 °C, 150 s. (LePera's etch).

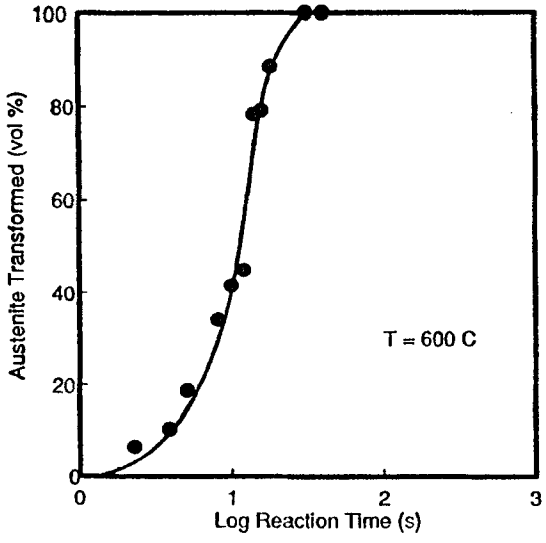

(*a*)

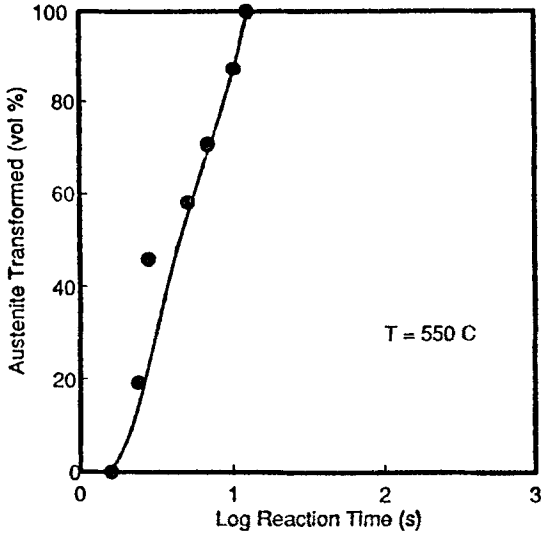

(*b*)

Fig. 7—Isothermal transformation curves for Fe-0.12 wt pct C-3.28 wt pct Ni: (*a*) bainite, transformed at 600 °C and (*b*) bainite, transformed at 550 °C.

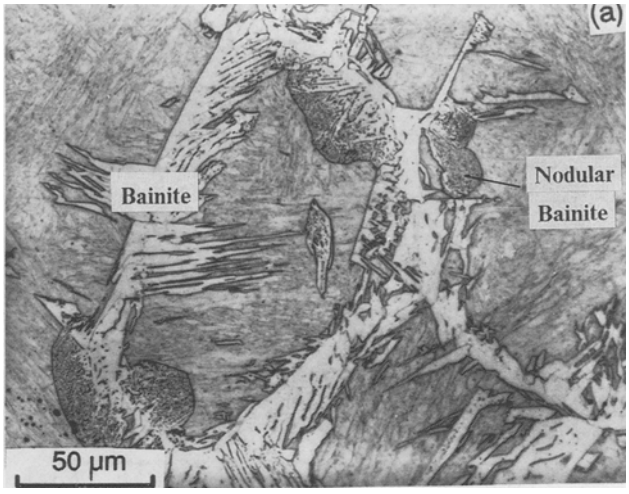

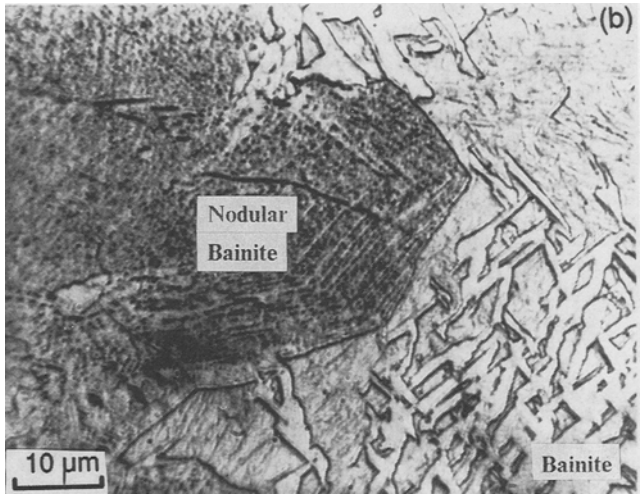

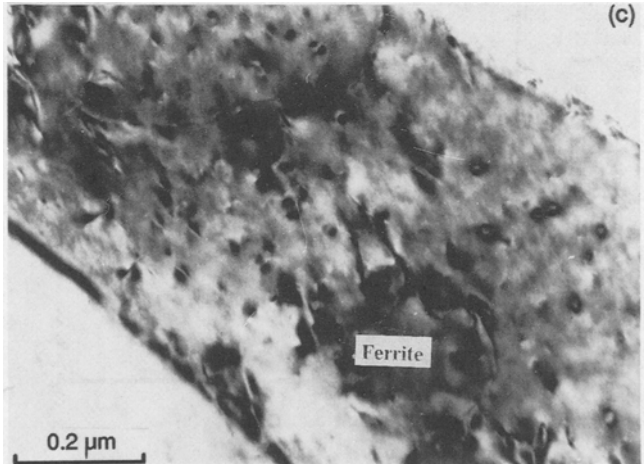

Fig. 8—Fe-0.12 wt pct C-3.28 wt pct Ni, transformed at 550 °C: (*a*) 5 s, optical microstructure; (*b*) 7 s, nodular bainite with interphase boundary carbides (2 pct nital pre-etch, LePera's etch); and (*c*) 5 s, TEM microstructure of carbide-free ferrite sideplates.

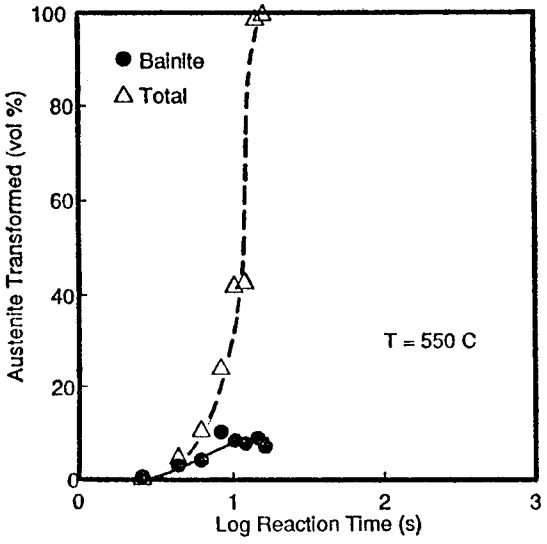

(*a*)

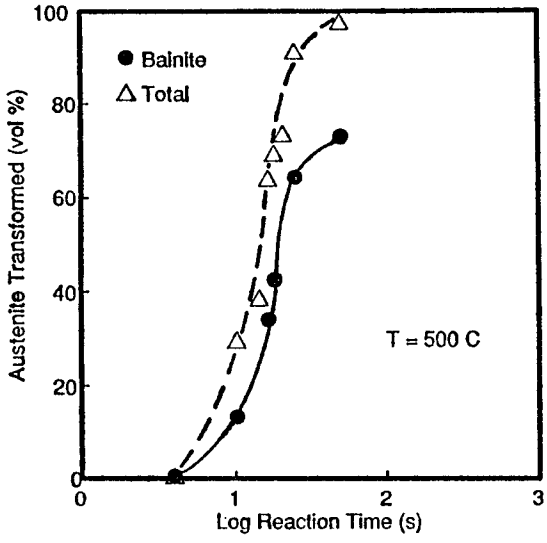

(*b*)

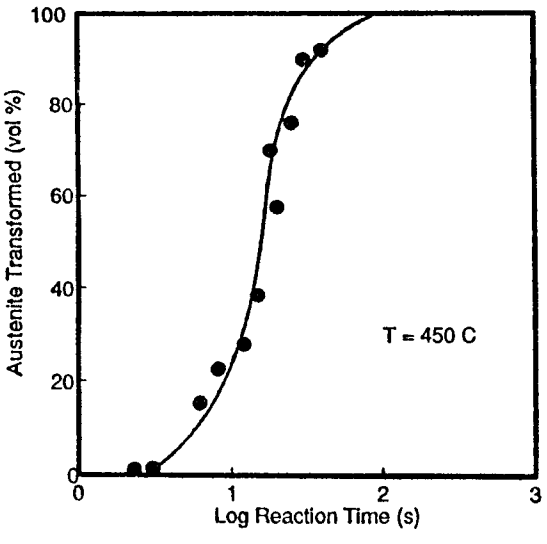

(*c*)

Fig. 9—Isothermal transformation curves for Fe-0.41 wt pct C-3.01 wt pct Cu: (*a*) bainite and total austenite reacted, transformed at 550 °C; (*b*) bainite and total austenite reacted, transformed at 500 °C; and (*c*) bainite and total austenite reacted, transformed at 450 °C.

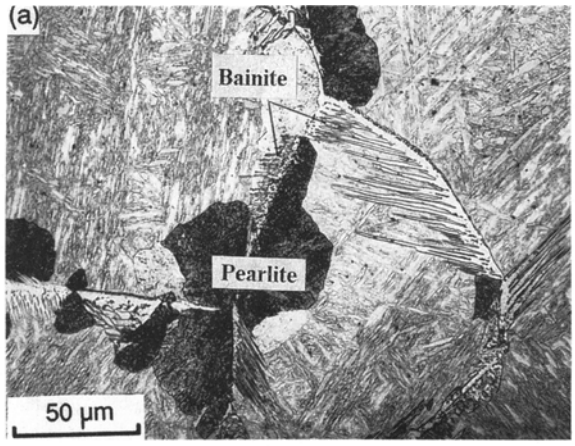

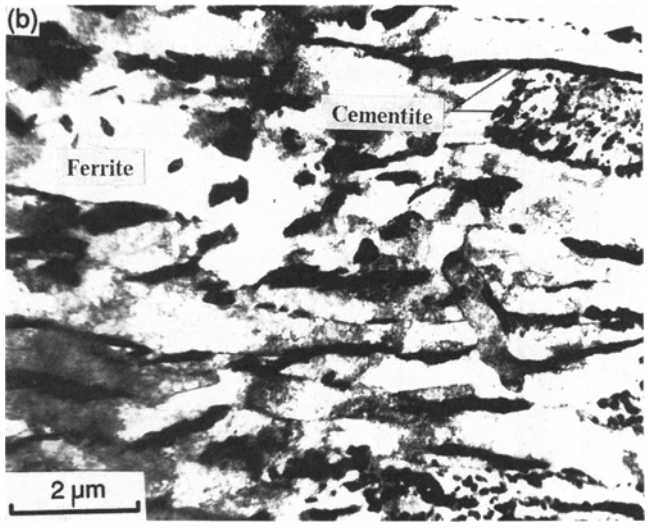

Fig. 10—Fe-0.41 wt pct C-3.01 wt pct Cu, transformed at 500 °C: (*a*) 10 s, optical microstructure (2 pct nital etch) and (*b*) 24 s, TEM microstructure.

450 °C and 400 °C, the second stage is no longer present; transformation occurs rapidly with no indication of incompleteness.

IV. DISCUSSION

Transformation stasis was not observed in most of the alloys investigated. Thus, incomplete transformation is evidently not a general characteristic of the bainite reaction, and the use of this phenomenon as a defining trait of bainite is clearly unjustified. The nature of the substitutional solute element does, however, play a significant role in the appearance of the incomplete transformation phenomenon. For example, incomplete transformation is not observed in the Fe-C-Si, Fe-C-Ni, or Fe-C-Cu alloys studied, but it is observed in the lower carbon Fe-C-Mn alloy and also has been observed in many Fe-C-Mo alloys.[9] The Wagner interaction parameters of Si, Ni, and Cu are all either positive or near zero,[24,25] so these elements either increase or have little effect on the activity of carbon in ferrite and austenite. On the other hand, Mn and particularly Mo lower the activity of carbon.[24,25] These observations are consistent with

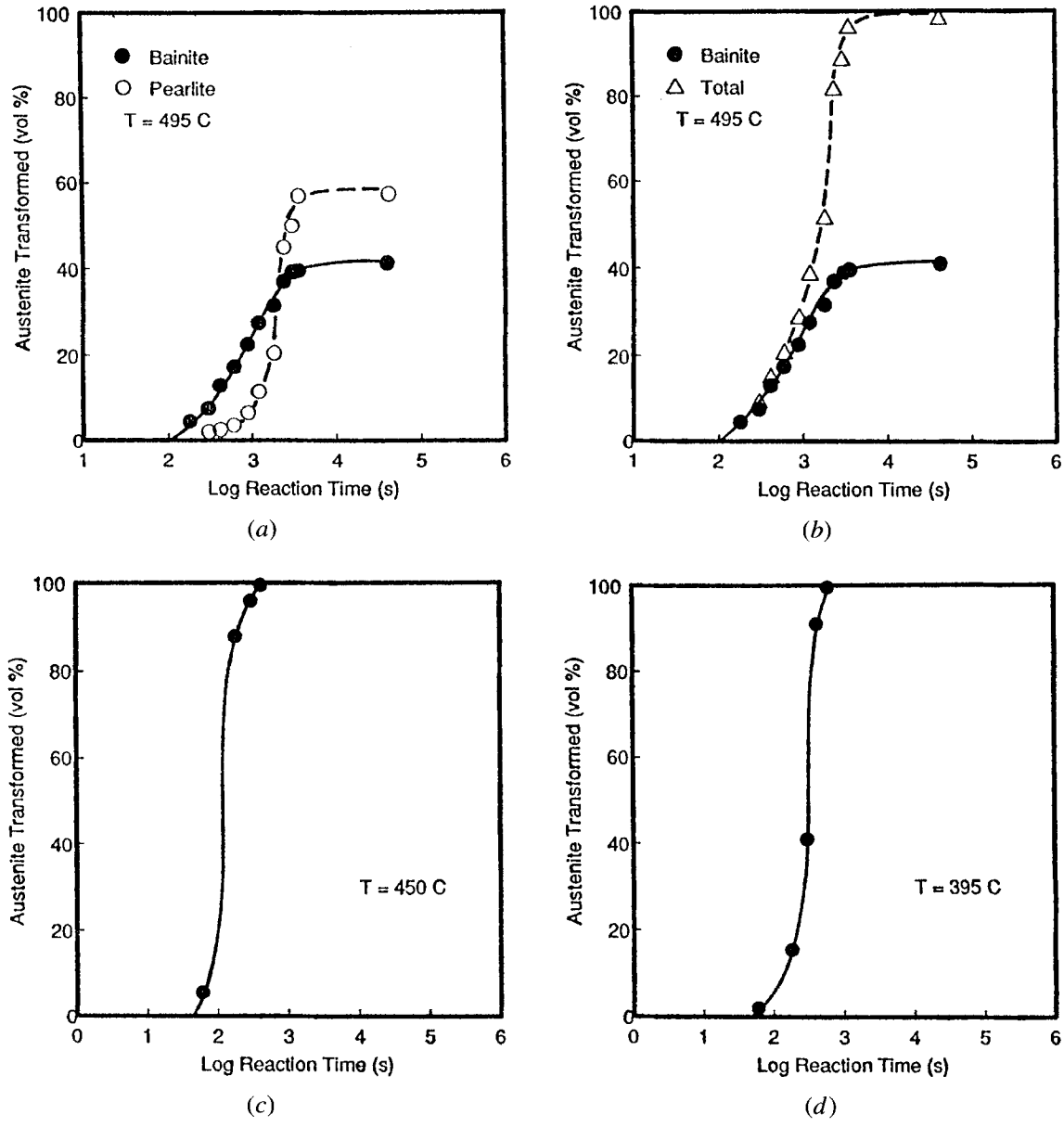

Fig. 11—Isothermal transformation curves for Fe-0.38 wt pct C-3.11 wt pct Mn:[35] (*a*) bainite and pearlite, transformed at 495 °C; (*b*) bainite and total austenite reacted, transformed at 495 °C; (*c*) bainite, transformed at 450 °C; and (*d*) bainite, transformed at 395 °C.

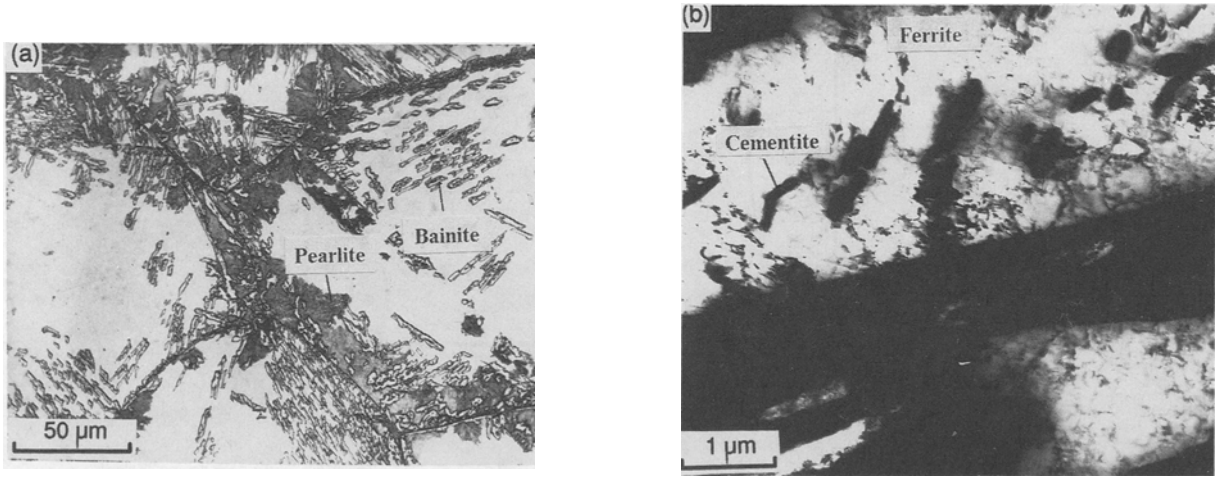

Fig. 12—Fe-0.38 wt pct C-3.11 wt pct Mn, transformed at 495 °C, 1800 s: (*a*) optical microstructure (2 pct nital etch) and (*b*) TEM microstructure.

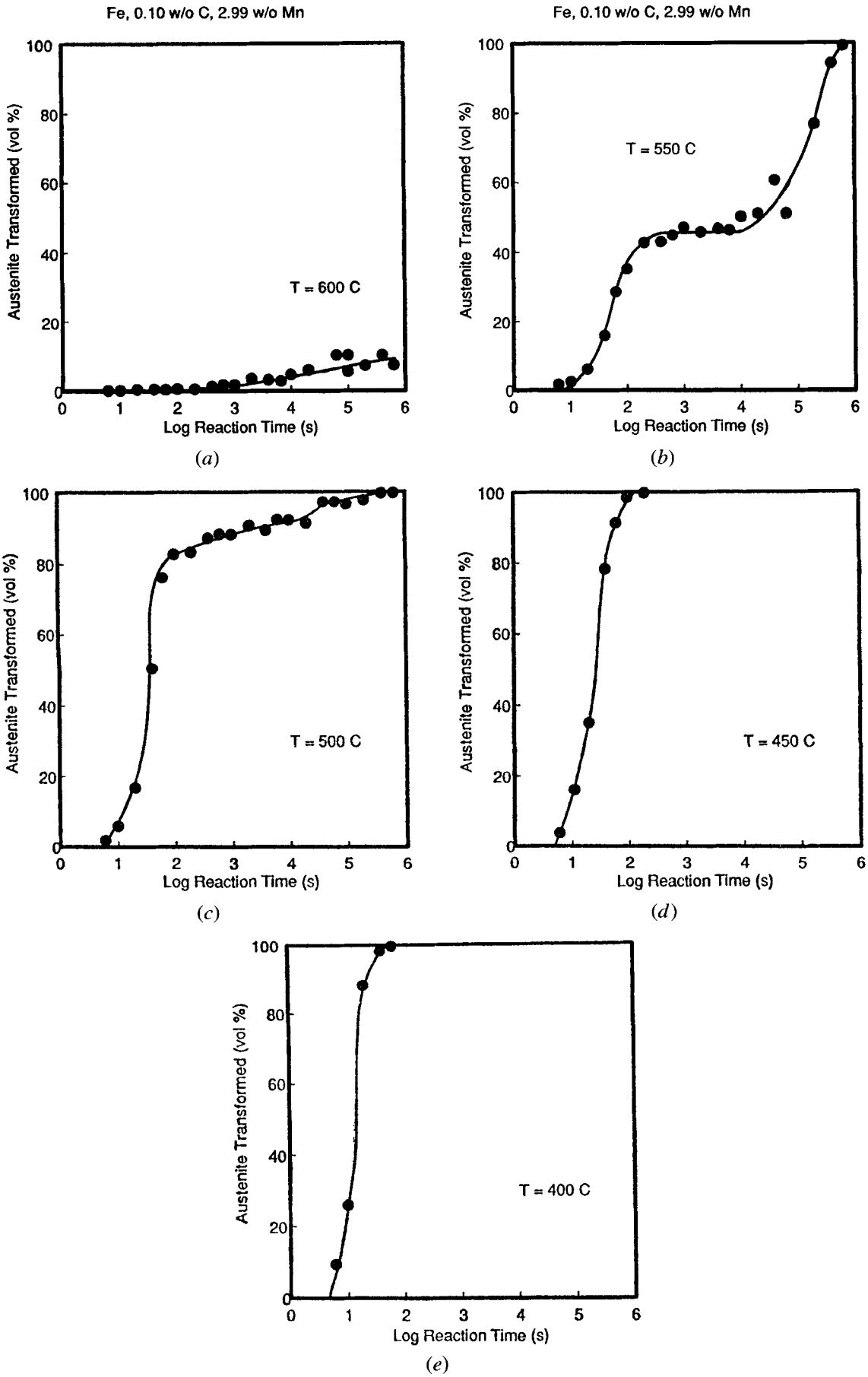

Fig. 13—Isothermal transformation curves for Fe-0.10 wt pct C-2.99 wt pct Mn: (*a*) bainite, transformed at 600 °C; (*b*) bainite, transformed at 550 °C; (*c*) bainite, transformed at 500 °C; (*d*) bainite, transformed at 450 °C; and (*e*) bainite, transformed at 400 °C.

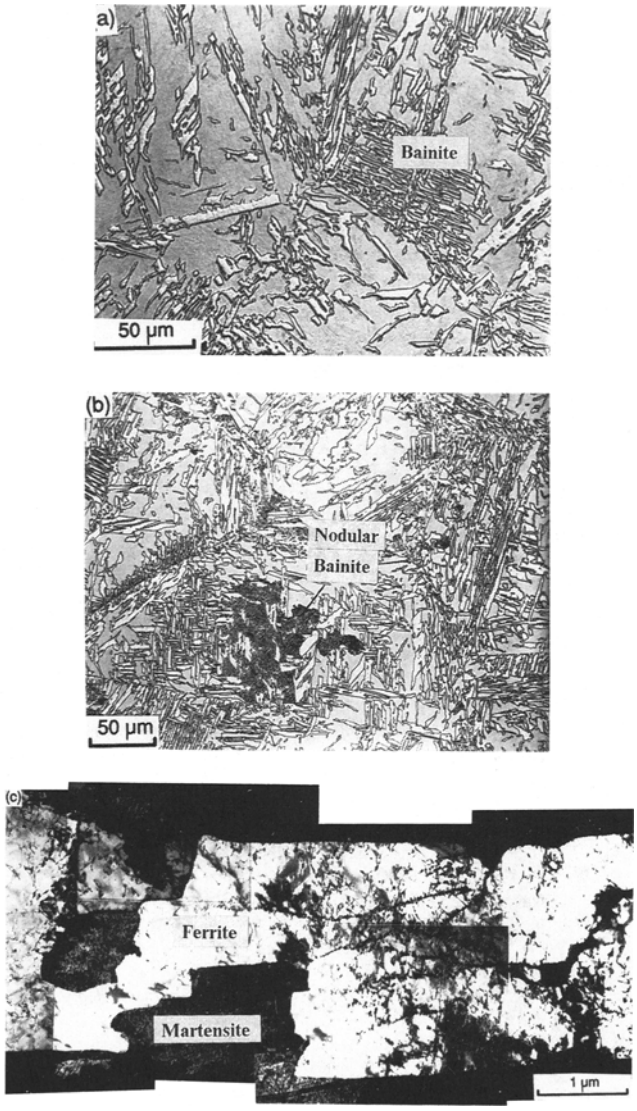

Fig. 14—Fe-0.10 wt pct C-2.99 wt pct Mn, transformed at 550 °C for (*a*) 20,000 s (during transformation stasis), optical microstructure; (*b*) 100,000 s (after transformation stasis), optical microstructure (LePera's etch); and (*c*) 1000 s (during transformation stasis), TEM microstructure.

the view that incomplete transformation is a manifestation of the SDLE. In a current model for this effect,[9] ferrite growth will take place at rates slower than those permitted by carbon diffusion with paraequilibrium boundary conditions whenever the chemical potential of carbon in the $\alpha:\gamma$ boundary is lower than the paraequilibrium value. Although this circumstance depends upon both the C and X concentrations in the boundary, it is more likely to occur if the substitutional solute lowers the C activity.

It has been suggested[9] that transformation stasis will occur under the following conditions: the SDLE must be strong enough to restrict ferrite growth and extensive carbide precipitation must be absent. The first condition encourages the renucleation of ferrite at stationary areas of $\alpha:\gamma$ boundaries at sufficiently high driving forces. This mode of nucleation, termed sympathetic nucleation,[48,49] becomes viable at temperatures below the B_s. Sympathetic nucleation produces the ferrite sheaves and the degenerate-appearing ferrite morphologies[22,50] often associated with kinetically defined bainite. The SDLE provides a barrier to ferrite growth and thus makes renucleation necessary for the transformation to proceed. The reaction is envisaged to occur by the nucleation of a ferrite crystal, growth of the ferrite until the SDLE stops the migration of the $\alpha:\gamma$ boundaries, and then nucleation of a new ferrite crystal at the stationary boundary. When carbide precipitation does not occur, the formation of ferrite is necessarily accompanied by carbon enrichment of the austenite adjacent to the ferrite crystals. The higher carbon concentration in this austenite lowers the driving force for sympathetic nucleation of ferrite, and transformation stasis results when sympathetic nucleation ceases.[9] Stasis ends when carbide precipitation restores ferrite growth by relieving the SDLE and by locally increasing the supersaturation for ferrite growth.[8,9]

It is possible that a barrier to ferrite growth also arises from sources other than an SDLE. For instance, partially coherent ferrite:austenite boundaries are immobile[23,51] and must migrate by a ledge mechanism.[23,51–53] Substitutional solutes may influence the overall mobility of ferrite:austenite boundaries by affecting the formation kinetics of growth ledges. Alloying elements that inhibit ledge formation would in effect accentuate the interfacial structure barrier to $\alpha:\gamma$ boundary migration and severely retard ferrite growth. This appears to happen at the edges of ferrite plates but not at grain boundary ferrite allotriomorphs in high-Ni, Fe-C-Ni alloys.[54] However, regardless of the relative contributions of the SDLE and interfacial structure to the growth barrier, such a barrier is necessary for the development of transformation stasis. Without it, transformation can continue by the growth of existing ferrite crystals rather than requiring the repeated nucleation of new crystals.

Ferrite morphologies formed in the absence of an SDLE can be observed by comparing the optical microstructures of alloys which do not exhibit transformation stasis with those of alloys which do exhibit this phenomenon. Sideplates and intragranular plates of ferrite are observed to form readily in Fe-C-Si, Fe-C-Ni, and Fe-C-Cu alloys (Figures 2(a), 4, 6, 8, and 10(a)). In the Fe-C-Mn alloys, where an SDLE is expected because Mn reduces the activity of carbon,[24,25] ferrite growth is much more restricted. As can be seen in Figures 12 and 14(a) and (b), the ferrite has a degenerate morphology[23] and plates only develop through the agency of repeated edge-to-edge sympathetic nucleation.[48,49] The circumstance that incomplete transformation is observed in the 0.10 pct C Fe-C-Mn alloy but not in the 0.38 pct C Fe-C-Mn alloy can be explained by the relative rates of carbide precipitation in these alloys. In the 0.38 pct C alloy, carbide precipitation occurs in conjunction with degenerate ferrite precipitation at the temperatures studied (Figure 12(b)). This condition limits the loss of supersaturation for ferrite nucleation due to the carbon enrichment of austenite by incorporating some of this carbon into the carbides. In the lower carbon alloy, carbide precipitation at ferrite:austenite boundaries is delayed considerably (Figure 14(c)), evidently because of the higher average growth rate of ferrite caused by the higher driving force for ferrite formation. The survival time of the

immobile terraces of growth ledges is thus reduced, thereby diminishing the nucleation kinetics of carbides at these terraces.[55] With carbides unavailable to act as sinks for the carbon rejected during ferrite precipitation, the carbon concentration in austenite increases more rapidly and diminishes the sympathetic nucleation kinetics of ferrite. In the presence of a sufficiently strong SDLE (perhaps supplemented by interfacial structure barriers to growth), transformation stasis can develop. The stasis regime lasts until carbide precipitation begins and the remainder of the austenite decomposes to the nodular eutectoid product (Figure 14(b)).

The presence of transformation stasis in a ternary alloy thus depends upon the effectiveness of the X element in inhibiting ferrite growth *and* upon its effect on carbide precipitation. Transformation behavior in quaternary or higher order alloys also should depend upon these factors. However, individual alloying elements may selectively alter ferrite growth or carbide precipitation and lead to synergism when introduced in the proper combinations. For example, an element which greatly depresses ferrite growth kinetics, such as Mo or Cr, also tends to be a carbide former. Combinations of two carbide formers can thus discourage transformation stasis if carbides form too readily or quickly. Combining a noncarbide former, such as Si or Ni, with Mo or Cr may actually encourage or accentuate transformation stasis if Mo or Cr continue to impede ferrite growth in the quaternary alloy and the Si or Ni delays carbide precipitation. Combinations of substitutional alloying elements may also alter the behavior of a given X element in the context of the SDLE. Such an effect may occur in Mn-Si steels in which Si has been suggested to increase Mn adsorption at $\alpha:\gamma$ boundaries and its resulting SDLE.[35]

Finally, the present results also reveal some of the inherent problems which result from identifying bainite by its kinetic features. In most of the alloys investigated, neither a well-defined B_s temperature nor transformation stasis is observed. However, bainite can be unambiguously identified by its microstructure.[7,56] On this approach, the term "bainite" is reserved for a nonlamellar, noncooperative mixture of ferrite and carbides formed during eutectoid decomposition. The carbide-free ferrite which precipitates at low temperatures in some Fe-C-X alloys, particularly Fe-C-Si, is properly identified as proeutectoid ferrite.

V. SUMMARY

1. The overall reaction kinetics of the bainite transformation were measured with quantitative optical metallography in Fe-C-X alloys to determine the presence or absence of the incomplete transformation phenomenon. The following alloys did not exhibit the incomplete transformation phenomenon: Fe-0.4 wt pct C-3 at. pct Si, Cu or Mn, Fe-0.4 wt pct C-6.8 at. pct Ni, and Fe-0.38 wt pct C-3 at. pct Mn.
2. The incomplete transformation phenomenon is not a general characteristic of the bainite transformation in Fe-C-X alloys.
3. The present results are consistent with the mechanism for the incomplete transformation phenomenon proposed in a companion paper on transformation kinetics in Fe-C-Mo alloys.[9]

ACKNOWLEDGMENTS

This work was made possible by financial support from the Army Research Office, the Metallurgical Engineering and Materials Science Department of Carnegie Mellon University, the American Iron and Steel Institute, the Electric Power Research Institute, the Office of Naval Research, the National Science Foundation, and the Air Force Office of Scientific Research, all of whose contributions are gratefully acknowledged.

REFERENCES

1. J.M. Robertson: *J. Iron Steel Inst.*, 1929, vol. 119, pp. 391-419.
2. H. Jolivet: *J. Iron Steel Inst.*, 1939, vol. 140, pp. 95-114.
3. W.T. Griffiths, L.B. Pfeil, and N.P. Allen: *Second Report of the Alloy Steels Research Committee*, The Iron and Steel Institute, London, 1939, pp. 343-67.
4. R.F. Hehemann and A.R. Troiano: *Met. Prog.*, 1956, vol. 70, pp. 97-104.
5. E.S. Davenport: *Trans. ASM*, 1939, vol. 27, pp. 837-86.
6. R.F. Hehemann: *Phase Transformations*, ASM, Metals Park, OH, 1970, pp. 397-432.
7. H.I. Aaronson: *The Mechanism of Phase Transformations in Crystalline Solids*, Institute of Metals, London, 1969, pp. 270-81.
8. G.J. Shiflet and H.I. Aaronson: *Metall. Trans. A*, 1990, vol. 21A, pp. 1413-32.
9. W.T. Reynolds, Jr., F.Z. Li, C.K. Shui, and H.I. Aaronson: *Metall. Trans. A*, 1990, vol. 21A, pp. 1433-63.
10. H.I. Aaronson, W.T. Reynolds, Jr., G.J. Shiflet, and G. Spanos: *Metall. Trans. A*, 1990, vol. 21A, pp. 1343-80.
11. F. Wever and H. Lange: *Mitt. Kaiser-Wilhelm-Inst. Eisenforsch.*, 1932, vol. 14, pp. 71-83.
12. H. Lange and K. Mathieu: *Mitt. Kaiser-Wilhelm-Inst. Eisenforsch.*, 1938, vol. 20, pp. 125-34.
13. A. Rose and W. Fischer: *Mitt. Kaiser-Wilhelm-Inst. Eisenforsch.*, 1939, vol. 21, p. 133.
14. F. Wever and K. Mathieu: *Mitt. Kaiser-Wilhelm-Instit. Eisenforsch.*, 1940, vol. 22, pp. 9-18.
15. N.P. Allen, L.B. Pfeil, and W.T. Griffiths: *Second Report of the Alloy Steels Research Committee*, The Iron and Steel Institute, 1939, pp. 369-90.
16. E.P. Klier and T. Lyman: *Trans. AIME*, 1944, vol. 158, pp. 394-419.
17. R.F. Hehemann, K.R. Kinsman, and H.I. Aaronson: *Metall. Trans.*, 1972, vol. 3, pp. 1077-94.
18. A.R. Troiano: *Trans. ASM*, 1949, vol. 41, pp. 1093-1107.
19. M. Enomoto and H.I. Aaronson: *Metall. Trans. A*, 1986, vol. 17A, pp. 1385-97.
20. K.R. Kinsman and H.I. Aaronson: *Transformation and Hardenability in Steels*, Climax Molybdenum Co., Ann Arbor, MI, 1967, pp. 39-53.
21. J.R. Bradley and H.I. Aaronson: *Metall. Trans. A*, 1981, vol. 12A, pp. 1729-41.
22. P.G. Boswell, K.R. Kinsman, G.J. Shiflet, and H.I. Aaronson: in *Mechanical Properties and Phase Transformations in Engineering Materials*, S.D. Antolovich, R.O. Ritchie, and W.W. Gerberich, eds., TMS-AIME, Warrendale, PA, 1986, pp. 445-66.
23. H.I. Aaronson: in *The Decomposition of Austenite by Diffusional Processes*, V.F. Zackay and H.I. Aaronson, eds., Interscience, New York, NY, 1962, pp. 387-546.
24. B. Uhrenius: in *Hardenability Concepts with Applications to Steel*, D.V. Doane and J.S. Kirkaldy, eds., TMS-AIME, Warrendale, PA, 1978, pp. 28-81.
25. J.S. Kirkaldy, B.A. Thomson, and E.A. Baganis: in *Hardenability Concepts with Applications to Steel*, D.V. Doane and J.S. Kirkaldy, eds., TMS-AIME, Warrendale, PA, 1978, pp. 82-125.

26. D.A. Scott, W.M. Armstrong, and F.A. Forward: *Trans. ASM*, 1949, vol. 41, pp. 1145-64.
27. J.P. Sheehan, C.A. Julien, and A.R. Troiano: *Trans. ASM*, 1949, vol. 41, pp. 1165-81.
28. M. Umemoto, T. Furuhara, and I. Tamura: *Acta Metall.*, 1986, vol. 34, pp. 2235-45.
29. J.R. Bradley, T. Abe, and H.I. Aaronson: *Rev. Sci. Instrum.*, 1982, vol. 53, pp. 98-99.
30. E.S. Davenport, R.A. Grange, and R.J. Hafsten: *Trans. AIME*, 1941, vol. 145, pp. 301-10.
31. H.I. Aaronson: *Trans. AIME*, 1958, vol. 212, pp. 212-18.
32. T. Gladman and J.H. Woodhead: *J. Iron Steel Inst.*, 1960, vol. 194, pp. 189-93.
33. J.E. Hilliard and J.W. Cahn: *Trans. AIME*, 1961, vol. 221, pp. 344-52.
34. C.K. Shui, W.T. Reynolds, Jr., G.J. Shiflet, and H.I. Aaronson: *Metallography*, 1988, vol. 21, pp. 91-102.
35. S.K. Liu, W.T. Reynolds, Jr., H. Hu, G.J. Shiflet, and H.I. Aaronson: *Metall. Trans. A*, 1985, vol. 16A, pp. 457-66.
36. M. Hillert and L.I. Staffansson: *Acta Chem. Scand.*, 1970, vol. 24, pp. 3618-26.
37. M. Hillert: *Jernkontorets Ann.*, 1952, vol. 136, pp. 25-37.
38. J.B. Gilmour, G.R. Purdy, and J.S. Kirkaldy: *Metall. Trans.*, 1972, vol. 3, pp. 1455-64.
39. H.J. Lee, G. Spanos, G.J. Shiflet, and H.I. Aaronson: *Acta Metall.*, 1988, vol. 36, pp. 1129-40.
40. W.T. Reynolds, Jr., F.Z. Li, C.K. Shui, G.J. Shiflet, and H.I. Aaronson: in *Phase Transformations 87*, G.W. Lorimer, ed., The Institute of Metals, London, 1988, pp. 330-33.
41. G. Spanos: Carnegie Mellon University, Pittsburgh, PA, unpublished research, 1985.
42. J.M. Oblak and R.F. Hehemann: *Transformation and Hardenability in Steels*, Climax Molybdenum Co., Ann Arbor, MI, 1967, pp. 15-30.
43. K.R. Kinsman and H.I. Aaronson: *Transformation and Hardenability in Steels*, Climax Molybdenum Co., Ann Arbor, MI, 1967, pp. 33-38.
44. F.B. Pickering: *Transformation and Hardenability in Steels*, Climax Molybdenum Co., Ann Arbor, MI, 1967, pp. 109-29.
45. A. Hultgren: *Trans. ASM*, 1947, vol. 39, pp. 915-89.
46. H.I. Aaronson and H.A. Domian: *Trans. AIME*, 1966, vol. 236, pp. 781-96.
47. M. Enomoto and H.I. Aaronson: *Metall. Trans. A*, 1987, vol. 18A, pp. 1547-57.
48. H.I. Aaronson and C. Wells: *Trans. AIME*, 1956, vol. 206, pp. 1216-23.
49. E.S.K. Menon and H.I. Aaronson: *Acta Metall.*, 1987, vol. 35, pp. 549-63.
50. H. Tsubakino and H.I. Aaronson: *Metall. Trans. A*, 1987, vol. 18A, pp. 2047-60.
51. H.I. Aaronson, C. Laird, and K.R. Kinsman: *Phase Transformations*, ASM, Metals Park, OH, 1970, pp. 313-96.
52. K.R. Kinsman, E. Eichen, and H.I. Aaronson: *Metall. Trans. A*, 1975, vol. 6A, pp. 303-17.
53. G.R. Purdy: *Acta Metall.*, 1978, vol. 26, pp. 487-98.
54. W.T. Reynolds, Jr. and H.I. Aaronson: *Scripta Metall.*, 1985, vol. 19, pp. 1171-76.
55. H.I. Aaronson, M.R. Plichta, G.W. Franti, and K.C. Russell: *Metall. Trans. A*, 1978, vol. 9A, pp. 363-71.
56. H.I. Aaronson and H.J. Lee: *Scripta Metall.*, 1987, vol. 21, pp. 1011-16.